JGR Earth Surface

RESEARCH ARTICLE
10.1029/2023JF007230

Modeling Steady Grain Sorting in River Bifurcations

Niccolò Ragno[1], Marco Redolfi[1], Nicoletta Tambroni[2], and Marco Tubino[1]

[1]Department of Civil, Environmental and Mechanical Engineering, University of Trento, Trento, Italy, [2]Department of Civil, Chemical and Environmental Engineering, University of Genoa, Genova, Italy

Key Points:

- Grain sorting reduces water and sediment flux asymmetry between downstream bifurcates
- The less-carrying branch undergoes significant fining, which enhances its sediment transport capacity
- The overall bed composition of downstream branches is finer than that of the feeder channel

Supporting Information:

Supporting Information may be found in the online version of this article.

Correspondence to:

N. Ragno,
niccolo.ragno@unitn.it

Citation:

Ragno, N., Redolfi, M., Tambroni, N., & Tubino, M. (2023). Modeling steady grain sorting in river bifurcations. *Journal of Geophysical Research: Earth Surface*, *128*, e2023JF007230. https://doi.org/10.1029/2023JF007230

Received 24 APR 2023
Accepted 10 SEP 2023

Abstract A striking feature of rivers is their ability to sort the sediments composing them. One of the chief causes for grain sorting consists in the selective transport of different sizes moving downstream. This process can be substantially influenced by the presence of lateral topographic variations, as those produced by channel bifurcations, in which water and sediment are diverted between two smaller anabranches. In particular, field and laboratory observations have shown that the asymmetric flux distribution commonly observed in actual bifurcations is associated with a coarsening of the most-carrying branch. Here, equilibrium sorting in river bifurcations is addressed through a quasi-2D model. Differently from previous works, a fully physically based description of the processes tied to a heterogeneous sediment mixture is introduced. The main mechanisms consist in the lateral pull of sediment due to a sloping bed upstream the bifurcation, and the variation of transport capacity in downstream branches. The model indicates that grain sorting tends to reduce the degree of flux asymmetry between branches for increasing heterogeneity of the mixture. Moreover, the uneven discharge distribution is associated with a different bed surface composition, with bed coarsening of the dominating channel and fining of the other branch. The reduced sediment transport asymmetry and bed surface fining enhance the transport of fine material in the less-carrying branch, thus contributing to keep it morphologically active. Finally, the model predicts an overall fining of bed surface material with respect to the feeder channel.

Plain Language Summary River bifurcations occur when the main channel course splits into two secondary branches. The partition of sediments between these branches is essential to define whether bifurcations are morphologically stable in time, preventing sedimentation, and abandonment of the smaller channel. In this paper, we formulate a mathematical model to study how sediments of different sizes divide at bifurcations in morphodynamic equilibrium. Specifically, we consider two classes of sediment particles (e.g., fine and coarse gravel) and we investigate the role of the key mechanisms driving the sediment transport: the gravitational effect, which tends to move downhill coarse particles; and the selective transport effect, which promotes the mobility of coarse particles within the most-carrying branch. These two mechanisms are found to bring contrasting effects, but the net results are clear. First, flow asymmetry is found to reduce with respect to the case where sediment particles of uniform size are considered. Second, the bed composition of the smaller branch becomes finer, contributing to maintain a significant sediment transport. These effects can explain patterns observed in gravel-bed river bifurcations, and suggest how adjustments of bed composition can contribute to maintaining all branches active in the long term.

1. Introduction

It is a longstanding recognition that rivers tend to sort the sediment they carry. In an insightful review paper on sediment sorting in 1991 Gary Parker wrote: "The decade of the 1980's saw a major change in thinking concerning sediment transport in rivers. Until that decade, research tended to be focused on uniform material. […] In the course of the 1980's, however, many of the important problems involving mixtures were at least formulated correctly. […] The writer expects that the 1990's will prove to be a decade in which the present understanding of the transport of mixtures will grow, and lead to a mechanistic explanations of most of the morphological consequences" (Parker, 1991b). After nearly 30 years, we can safely state that the wish of Parker has been substantially fulfilled. The attention devoted by the scientific community to various morphodynamic problems closely related to grain sorting is well portrayed by a number of experimental, numerical and field results. Among the morphological consequences discussed by Parker, we can recall the static and mobile armoring usually observed in gravel-bed rivers (e.g., Parker & Klingeman, 1982; Parker & Sutherland, 1990), the formation of longitudinal streaks of sediment and sorting waves known as bedload sheets (e.g., Colombini & Parker, 1995; Iseya & Ikeda, 1987; Seminara et al., 1996; Whiting et al., 1988), the sorting patterns in meandering and braided streams

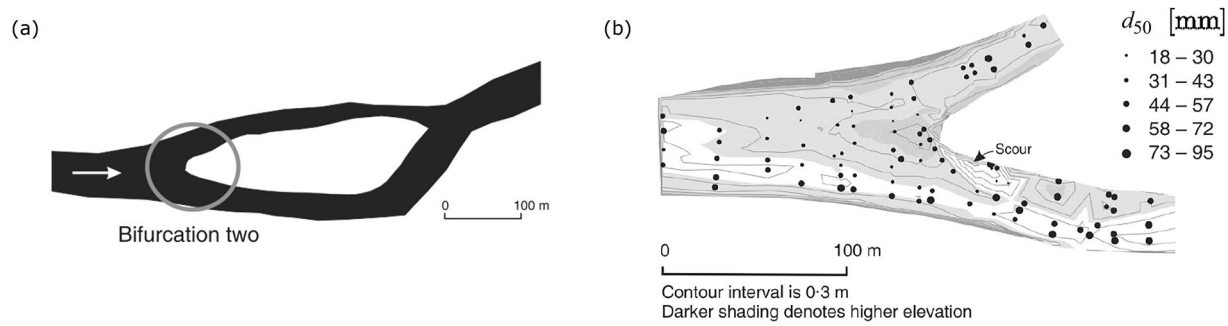

Figure 1. Example of a bifurcation-confluence unit on the Renous River (Canada) analyzed by Burge (2006): (a) planform view and (b) map of the spatial distribution of the median grain size at a bifurcation-confluence unit (adapted from his Figure 4). Bed coarsening in the wider and most-carrying right branch is clearly discernible.

(e.g., Ashworth et al., 1992; Ikeda, 1989; Parker & Andrews, 1985; Seminara et al., 1997; Sun et al., 2001), the sequences of "bar-flat" units in ephemeral streams (Powell et al., 2012), and the progressive downstream fining that arises due to the combined effect of selective deposition and grain abrasion (e.g., Cui et al., 1996; R. I. Ferguson et al., 1996; Hoey & Ferguson, 1994; Parker, 1991a; Paola & Seal, 1995; Paola et al., 1992).

A morphodynamic problem that was not explicitly mentioned in Parker's review is that of river bifurcations. This lack is somehow understandable, since the first attempt to describe river bifurcations through a morphodynamic model came some years later (Wang et al., 1995), despite some interesting analysis were already conducted, both theoretically and experimentally, by Kawai (1991). On the other hand, Parker recognized that a multi-thread morphology could have significant implications on grain sorting, in particular regarding downstream fining. Braided streams often display local lateral "patches" of sediment, each one with its own characteristic distribution (Paola & Seal, 1995). These patches can dominate the process of selective deposition, and thus the downstream decrease of grain size.

Little is known, however, about how grain size distribution may affect the sediment flux partition at individual bifurcations, which can be regarded as the basic units of multi-thread streams (e.g., Ashmore, 2013; Kleinhans et al., 2013; Ragno et al., 2021). The occurrence of sorting in natural bifurcations is highlighted by several field studies (Ashworth et al., 1992; Burge, 2006; Frings & Kleinhans, 2008; Kästner & Hoitink, 2019; Szewczyk et al., 2021), whereas laboratory experiments are restricted to a handful of works performed by Hasegawa and co-workers nearly 20 years ago (e.g., Hirose et al., 2003; Meguro et al., 2002). From these experiments, which were conducted with reference to a geometrically symmetric bifurcation, the tendency for a bed coarsening of the channel carrying the largest amount of water and sediment emerged. This behavior is consistent with the field-based analysis carried out by Burge (2006) on several bifurcation-confluence units in the gravel-bedded Renous River, Canada (Figure 1). Despite the wealth of factors that may potentially affect flow and sediment discharge division in the field, the data collected by Burge (2006) showed that an unbalanced flux distribution at the bifurcation is associated with a different bed topography and sorting pattern. Specifically, the channel carrying the lowest amount of water and sediment is characterized by a higher bed elevation due to bar formation at the channel entrance, in turn preventing the coarser fraction of sediment to be carried downstream in that branch.

The majority of theoretical models of river bifurcations developed so far focused on the case of uniform material. The only exception the writers are aware of is the recent analysis performed by Schielen and Blom (2018), which follows a straightforward generalization of the Wang et al. (1995) model. In addition to the limitations embedded in this model, in which sediment partitioning relies on an empirical parameter strongly dependent on the transport formula adopted, Schielen and Blom (2018) neglect several basic, yet fundamental mechanisms closely tied to grain sorting. In particular, both the so-called hiding effect, which reduces the differences in mobility between heavier and lighter grains, and the dependence on grain size of gravitational force on the lateral sediment transport are discarded.

It is now fairly recognized that the gravitational pull along transverse bed slopes represents a key effect determining bifurcation evolution, at least in gravel-bed streams (Bolla Pittaluga et al., 2003). In the case of mixtures the picture becomes more complex, since it is still unclear what is the role of grain exposure and hiding on the lateral transport of different grain sizes (Kleinhans et al., 2013; Sloff & Mosselman, 2012). So far, two different

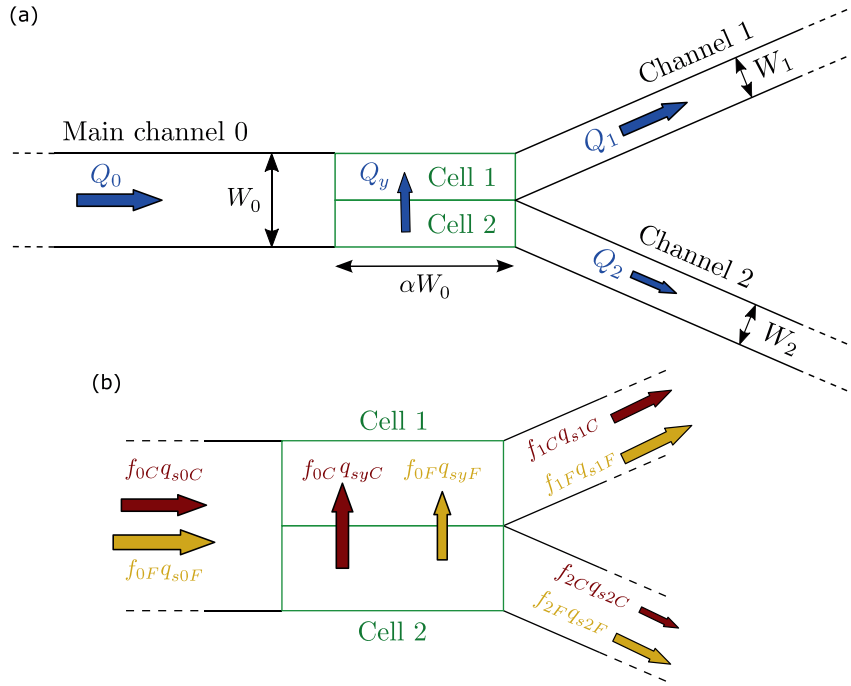

Figure 2. Sketch of the free bifurcation model. (a) Plan view, where arrows indicate the water fluxes within the channel and between the nodal cells; (b) detail of sediment fluxes for the fine (yellow) and the coarse (dark red) fractions. Without loss of generality, we assume that most of water and sediment is flowing toward the left branch (channel 1).

recipes can be found in the literature, though with a lack of a sound mechanistic justification: a first approach assumes that hiding also affects the transport direction (e.g., Lanzoni & Tubino, 1999; Nelson et al., 2015; Parker & Andrews, 1985); differently, other works neglect the effect of hiding by assuming that the transverse downslope movement depends on the different weight of grain sizes composing the mixture (e.g., Cordier et al., 2019; Singh et al., 2017).

In this work we tackle the problem of grain sorting in river bifurcations with the inspiring words of Parker in mind. The main issues we intend to address are: why does the bed coarsen in the most-carrying branch form? What are the key mechanisms controlling this behavior? What is the role of hiding on lateral sorting? Can bifurcations enhance downstream fining in a multi-thread morphology? In order to answer these questions, a suitable treatment of sediment mixtures for a *free* (i.e., geometrically symmetric with no external effects) bifurcation is incorporated within the widely employed modeling framework of Bolla Pittaluga et al. (2003) (hereafter denoted with the acronym BRT). The attention is restricted to the case of gravel-bed rivers.

2. Formulation of the Problem

Let the scheme illustrated in Figure 2a be considered, where a main channel of width W_0 splits in two branches of width $W_1 = W_2 = W_0/2$. The main channel is fed by constant water and sediment supply. The BRT two-cell approach allows for considering, in a simplified manner, the two-dimensional topographical effects that physically manifest just upstream the bifurcation through the formation of a steady alternate bar (see e.g., Redolfi et al., 2019 for more details). Here, the key difference with respect to the classical BRT scheme consists in assuming a river bed surface that is composed by a mixture of sediment distributed according to the probability density $f(\phi)$, where ϕ is the sedimentological scale for particle size. Specifically, if d denotes a generic grain size, then ϕ is defined such that:

$$\phi = -\log_2(d/d_{ref}), \tag{1}$$

with d_{ref} conventionally set to 1 mm. Note that the use of the word surface is not of secondary importance. Indeed, it is assumed that the sediment available for transport is embedded in a superficial *active layer* (Hirano, 1971),

which is typically coarser than the substrate (Parker & Klingeman, 1982). Accordingly, the transport relations that will be adopted are surface-based.

We focus on the steady state configurations of the system. Therefore, following BRT formulation we consider all the variables (flow depth, velocity, grain size distribution) to be spatially uniform within each channel, with the exception of the area just upstream the bifurcation node.

With reference to Figure 2a, let f_i ($i = 0, 1, 2$) denote the grain size distribution in each channel i. The corresponding values of geometric mean grain size d_{gi} and standard deviation σ_{gi} are then given by:

$$d_{gi} = d_{ref} 2^{-\phi_{mi}}, \qquad \sigma_{gi} = 2^{\sigma_i}, \tag{2}$$

where ϕ_{mi} and σ_i are defined as:

$$\phi_{mi} = \int_{-\infty}^{+\infty} f_i \phi \, d\phi, \qquad \sigma_i^2 = \int_{-\infty}^{+\infty} f_i (\phi - \phi_{mi})^2 d\phi. \tag{3}$$

The volumetric sediment flux per unit width in each channel, q_{si}, is then computed as:

$$q_{si} = \int_{-\infty}^{+\infty} f_i q_{si\phi} \, d\phi. \tag{4}$$

If we consider bedload only, a general relation for the transport rate $q_{s\phi}$ of grain size ϕ can be expressed in the following form (e.g., Parker, 1990; Parker & Klingeman, 1982):

$$q_{s\phi} = \frac{(\tau/\rho)^{3/2}}{g\Delta} \mathcal{G}(\zeta), \qquad \zeta = g_{hr} \frac{\theta_g}{\theta_r}, \tag{5}$$

where θ_g is the Shields mobility number:

$$\theta_g = \frac{\tau}{\rho g \Delta d_g}, \tag{6}$$

and θ_r is the reference value of Shields number for sediment motion, τ is the bottom shear stress, g is the gravity acceleration, ρ is the water density, and Δ is the relative submerged weight of sediment. Various expressions for the transport function $\mathcal{G}(\zeta)$ have been proposed through the years (e.g., Ashida & Michiue, 1972; Parker, 1990; Powell et al., 2001; Wilcock & Crowe, 2003). Regardless of its explicit expression, the fundamental aspect is that $\mathcal{G}(\zeta)$ accounts for the different mobility of individual grain sizes through the reduced hiding function $g_{hr} = \mathcal{F}(d_g/d)$.

Since the seminal work by Einstein (1950), it is well known that the transport of mixtures is affected by two competing mechanisms. On one hand, larger grains are harder to be moved as they are heavier than finer grains. If this mechanism is the only one at play, it would imply that every grain in the mixture would act as if it is surrounded by grains of the same size (Parker, 2004). It follows that accounting just for the different weight of sediment would lead g_{hr} to be simply proportional to the ratio d_g/d, a condition that is typically called "grain (or gradation) independence" (Parker & Klingeman, 1982). On the other hand, grains in mixtures actually feel their neighbors. Fine grains tend to be shielded by coarse grains, which in turn protrude more into turbulent flow and thus are subject to a higher fluid drag (Egiazaroff, 1965; Einstein, 1950; Parker, 2008). The effect of hiding then partially compensates for the weighting d_g/d toward fine grains (Parker, 1991b). This mechanism allows to define a second limiting case, that is the so-called condition of "equal mobility" (i.e., $g_{hr} = 1$). It has been shown that most gravel-bed rivers tend to move the coarse and fine halves of the gravel load supplied to them at nearly the same rate, which is accomplished through the formation of a pavement layer (i.e., mobile armor) at the bottom surface (e.g., Parker & Klingeman, 1982; Parker & Toro-Escobar, 2002). Nevertheless, equal mobility is seldom achieved in a strict sense (e.g., Ashworth & Ferguson, 1989). The reduced hiding function g_{hr} is shown in Figure A1 of Appendix A, in accordance to some of the most-used expressions available in the literature.

The fundamental element of the BRT formulation consists in a nodal point relation that allows to predict how the incoming sediment flux q_{s0} is distributed between the downstream branches. The model is based on the application of sediment mass continuity equation to each nodal cell, accounting for the lateral exchange of sediment

driven by flow exchange and transverse slope. In the case of mixtures, it has been largely debated on how sorting mechanisms affect not only the transport capacity of the flow, but also the lateral transport. Indeed, on a sloping plane gravity tends to differently pull downhill sediment particles depending on their weight (Parker & Andrews, 1985; Yamasaka et al., 1987). The BRT nodal point relation can be readily amended following the expression proposed by Parker and Andrews (1985). We then compute the transverse flux (per unit length) $q_{sy\phi}$ of sediment of size ϕ in the form:

$$q_{sy\phi} = q_{s0\phi}\left[\frac{q_y}{q_0} - \frac{r}{\sqrt{\theta_{g0} l_{hr}}}\frac{(\eta_1 - \eta_2)}{W_0/2}\right], \tag{7}$$

where q_y is the lateral flow exchange (per unit length) between the two cells, q_0 is the incoming water discharge (per unit width), $\eta_{1,2}$ are the bed elevations at the inlet of the two downstream branches, and the parameter r is the Ikeda coefficient controlling the magnitude of the gravitational effect (Ikeda, 1982).

The function l_{hr} takes into account the dependence on grain size of the gravitational pull on the transversal exchange of sediment. The assumption that the effect of hiding must also be included in the function l_{hr} has been widely used in theoretical and numerical studies of sorting patterns in meandering rivers (Parker & Andrews, 1985; Sun et al., 2001) and alternate bars formation (Hasegawa et al., 2000; Lanzoni & Tubino, 1999; Nelson et al., 2015). Differently, other works have relied on the assumption of grain independence. This was done, among others, by Olesen (1987), Singh et al. (2017), Qian et al. (2017), and Cordier et al. (2019), yet without a mechanistic motivation. Nonetheless, Yamasaka et al. (1987) performed several experiments by means of a lateral tilting wind tunnel. Their results give some support to the reliability of the gradation independence assumption, in spite of the fact that just air flows were used.

In this paper, the transport function $\mathcal{G}$ and the reduced hiding function g_{hr} are computed using the expressions proposed by Wilcock and Crowe (2003):

$$\mathcal{G}(\zeta) = \begin{cases} 0.002\,\zeta^{7.5} & \text{if } \zeta < 1.35 \\ 14.2\left(1 - \frac{0.894}{\zeta^{0.5}}\right)^{4.5} & \text{if } \zeta \geq 1.35 \end{cases}, \tag{8a}$$

$$g_{hr} = \left(\frac{d}{d_{g0}}\right)^{-b}, \qquad b = \frac{0.67}{1 + \exp(1.5 - d/d_{g0})}, \tag{8b}$$

where a constant value of the reference Shields $\theta_r = 0.036$ is used, therefore assuming a gravel mixture without a significant presence of sand.

Regarding the function l_{hr}, we have tested both alternatives, namely $l_{hr} = g_{hr}$ or $l_{hr} = d_{g0}/d$ ("grain independence"), and found that the latter assumption leads to better agreement with field and laboratory observations, as will be further discussed in the text.

The system of nodal point conditions is then completed by assuming the water surface elevation at the bifurcation node to be the same in the three branches (i.e., $H_0 = H_1 = H_2$), and imposing the conservation of the water discharge:

$$q_1 + q_2 = 2\,q_0. \tag{9}$$

The flow rate q is expressed through the following uniform flow relation:

$$q = c\,D^{3/2}\sqrt{gS}, \qquad c = c(\phi, D), \tag{10}$$

where D is the flow depth and S is the channel slope, and the dimensionless Chézy coefficient c is assumed to depend on both the flow depth and the bed surface composition. Specifically, assuming the absence of small bedforms like ripples and dunes, the Chézy coefficient is expressed through the following logarithmic-type relation (e.g., Keulegan, 1938):

$$c = 6 + 2.5\log\left(\frac{D}{k_s}\right), \tag{11}$$

where the roughness height k_s depends on the diameter d_σ that represents the size of the coarser part of the grain size distribution (Parker, 1991b):

$$k_s = n_\sigma d_\sigma = n_\sigma d_g 2^\sigma, \tag{12}$$

with $n_\sigma \simeq 2$–3.5 (e.g., Parker, 2008).

Henceforth, we consider the simplest case of a bimodal mixture composed by a coarse component of size ϕ_C and fine part of size ϕ_F, whose proportion on the bed surface is indicated by f_C and $f_F = 1 - f_C$. Once applied to the two fractions, Equation 7 yields:

$$q_{syC} = q_{s0C}\left[\frac{q_y}{q_0} - \frac{r}{\sqrt{\theta_{g0} l_{hrC}}}\frac{(\eta_1 - \eta_2)}{W_0/2}\right], \tag{13a}$$

$$q_{syF} = q_{s0F}\left[\frac{q_y}{q_0} - \frac{r}{\sqrt{\theta_{g0} l_{hrF}}}\frac{(\eta_1 - \eta_2)}{W_0/2}\right], \tag{13b}$$

which constitute the basic nodal point relations. Taking the length of the nodal cells equals to αW_0 (see Figure 2), the lateral fluxes are related to the sediment transport within the channels through the following mass conservation equations:

$$q_y = \frac{1}{2\alpha}(q_1 - q_0), \tag{14a}$$

$$f_{0C} q_{syC} = \frac{1}{2\alpha}(f_{1C} q_{s1C} - f_{0C} q_{s0C}), \tag{14b}$$

$$f_{0F} q_{syF} = \frac{1}{2\alpha}(f_{1F} q_{s1F} - f_{0F} q_{s0F}), \tag{14c}$$

where, consistently with previous studies (e.g., Ragno et al., 2021), in the following a representative value $\alpha = 4$ is considered.

Summarizing, the generalization to the case of a bimodal mixture of the BRT model for a free bifurcation translates into the following system of nonlinear algebraic equations:

$$q_1 + q_2 = 2q_0, \tag{15a}$$

$$f_{1C} q_{s1C} = q_{s0C} f_{0C}\left[\frac{q_1}{q_0} - \frac{2r\alpha}{\sqrt{\theta_{g0} l_{hrC}}}\frac{(\eta_1 - \eta_2)}{W_0/2}\right], \tag{15b}$$

$$f_{1F} q_{s1F} = q_{s0F} f_{0F}\left[\frac{q_1}{q_0} - \frac{2r\alpha}{\sqrt{\theta_{g0} l_{hrF}}}\frac{(\eta_1 - \eta_2)}{W_0/2}\right], \tag{15c}$$

$$f_{1C} q_{s1C} + f_{2C} q_{s2C} = 2 f_{0C} q_{s0C}, \tag{15d}$$

$$f_{1F} q_{s1F} + f_{2F} q_{s2F} = 2 f_{0F} q_{s0F}, \tag{15e}$$

$$H_0 = H_1 = H_2. \tag{15f}$$

3. Linear Analysis

The system (15a–15f) admits of a trivial, balanced solution, in which water and sediment discharges are evenly distributed between the two branches, so that no exchange occurs between the two nodal cells, and the flow parameters and grain size distribution are the same throughout the domain and coincide with those of the upstream channel. It is well established that the stability of such balanced solution is primarily controlled by the (half) width-to-depth ratio (or aspect ratio) of the main channel $\beta_0 = W_0/(2D_0)$ (e.g., Bolla Pittaluga et al., 2003;

Redolfi et al., 2019). In particular, there exists a critical value β_{cr} for which a *pitchfork bifurcation* of the equilibrium diagram appears, so that for larger values of β_0 the trivial balanced solution becomes unstable, and two stable, unbalanced solutions emerge.

The marginal stability condition for which slightly unbalanced, steady solutions are possible can be found through a linear analysis of system (15a–15f) considering the balanced solution as the base state, which is then altered by adding an infinitesimal perturbation. We note that in the case of a sediment mixture the base state can be uniquely defined once the dimensionless parameters describing the hydraulic and sediment characteristics of the main upstream channel are assigned, namely β_0, θ_{g0}, d_{g0}, f_{0C}, and σ_0.

In practice, each dependent variable (say X) is expanded as follows:

$$X = X_0 + \delta\hat{X}, \qquad \delta \ll 1, \tag{16}$$

with δ indicating the order of magnitude of the perturbation. Substituting from Equation 16 into Equations 15a–15f, expanding in Taylor series and neglecting higher-order terms arising from nonlinear interactions, we obtain a linear system that can be expressed in terms of the unknowns $\hat{D}$ and $\hat{f}_C$ as follows:

$$\begin{pmatrix} a_{11} & a_{12} \\ a_{21} & a_{22} \end{pmatrix} \begin{pmatrix} \hat{D} \\ \hat{f}_C \end{pmatrix} = \begin{pmatrix} 0 \\ 0 \end{pmatrix}, \tag{17}$$

where the algebraic coefficients a_{ij} are given by:

$$a_{11} = q_{\eta C} - \left(\frac{3}{2} + c_D\right) - \frac{4r\alpha}{\beta_0\sqrt{\theta_{g0} l_{hrC}}}, \tag{18a}$$

$$a_{12} = q_{\phi C}(\phi_{0C} - \phi_{0F}) - c_\phi(\phi_{0C} - \phi_{0F}) - c_\sigma\sigma_f + \frac{1}{f_{0C}}, \tag{18b}$$

$$a_{21} = q_{\eta F} - \left(\frac{3}{2} + c_D\right) - \frac{4r\alpha}{\beta_0\sqrt{\theta_{g0} l_{hrF}}}, \tag{18c}$$

$$a_{22} = q_{\phi F}(\phi_{0C} - \phi_{0F}) - c_\phi(\phi_{0C} + \phi_{0F}) - c_\sigma\sigma_f - \frac{1}{f_{0C}}. \tag{18d}$$

Various coefficients appear in Equations 18a–18d. Specifically, c_D, c_ϕ, and c_σ measure the sensitivity of the Chézy coefficient to variations of flow depth and grain size distribution, being defined as follows:

$$c_D = \frac{1}{c_0}\frac{\partial c}{\partial D}\bigg|_{D_0}, \quad c_\phi = -\log(2)c_d, \quad c_\sigma = -c_\phi, \quad c_d = \frac{d_{g0}}{c_0}\frac{\partial c}{\partial d_g}\bigg|_{d_{g0}}. \tag{19}$$

The coefficients q_η and q_ϕ, which measure the sensitivity of the transport rate to variations of Shields number and grain size composition, read as:

$$q_\eta = \frac{3}{2} + \Gamma, \qquad q_\phi = \zeta_\phi\Gamma, \qquad \Gamma = \frac{\zeta_0}{\mathcal{G}_0}\frac{d\mathcal{G}}{d\zeta}\bigg|_0, \tag{20}$$

where:

$$\zeta_0 = \frac{\theta_{g0}}{\theta_r} g_{hr0}, \qquad \zeta_\phi = (g_{hrd} + 1)\log(2), \qquad g_{hrd} = \frac{1}{g_{hr0}}\frac{\partial g_{hr}}{\partial(d/d_g)}\bigg|_{d_{g0}}, \tag{21}$$

with g_{hrd} denoting the perturbation of the reduced hiding function due to grain size variations, and finally:

$$\sigma_f = \frac{\partial\sigma}{\partial f_C}\bigg|_0. \tag{22}$$

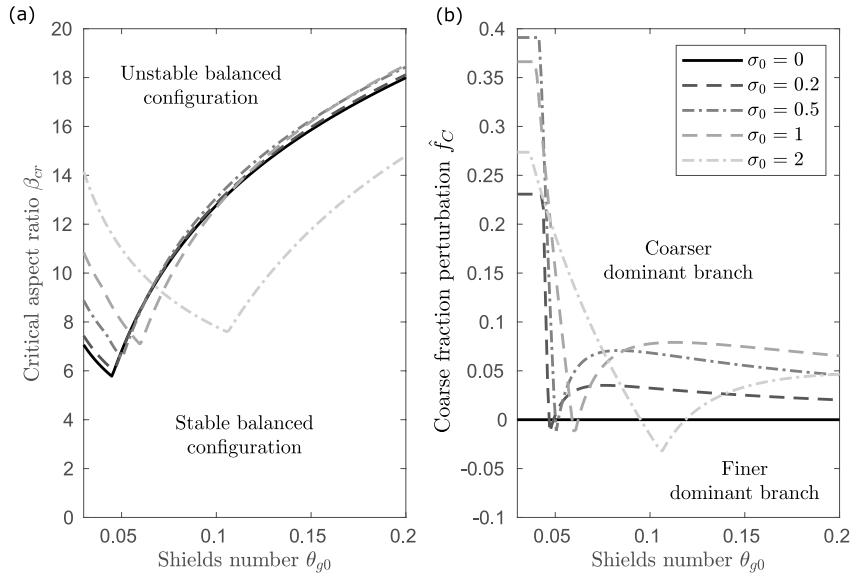

Figure 3. Outcomes of linear analysis depending on reference Shields number θ_{g0} for increasing values of the standard deviation σ_0. (a) Critical aspect ratio β_{cr} and (b) perturbation of the coarse fraction $\hat{f}_C$ in the dominant channel for a unitary depth perturbation $\hat{D} = 1$. The plots are shown for $d_{g0} = 0.02$.

A nontrivial solution of system (17) exists (i.e., $\hat{D} \neq 0$ and $\hat{f}_C \neq 0$) provided the determinant of the matrix of coefficients is different from zero. This allows for determining the marginal conditions for the stability of the bifurcation system, which can be cast into the following general functional form:

$$\mathcal{F}(\beta_{cr}, \theta_{g0}, d_{g0}, f_{0C}, \sigma_0) = 0. \tag{23}$$

From Equation 23, the following explicit expression for the critical aspect ratio β_{cr} is obtained:

$$\beta_{cr} = \frac{4r\alpha}{\sqrt{\theta_{g0}}}\left(\frac{a_{22}}{\sqrt{l_{hrC}}} - \frac{a_{12}}{\sqrt{l_{hrF}}}\right)\frac{1}{\left[\left(q_{\eta_C} - 3/2 - c_D\right)a_{22} - \left(q_{\eta_F} - 3/2 - c_D\right)a_{12}\right]}. \tag{24}$$

The values of the critical aspect ratio β_{cr} as predicted by Equation 24 are plotted in Figure 3a as a function of the Shields number θ_{g0} and for different values of the standard deviation σ_0, by assuming gradation independence along the lateral direction. Furthermore, the reference mixture is assumed to be composed of an equal amount of the two fractions, thus $f_{0C} = f_{0F} = 1/2$.

For $\sigma_0 = 0$ (i.e., uniform grain size), the critical aspect ratio β_{cr} generally increases with θ_{g0}, consistently with the result obtained through existing uniform sediment models for bifurcations in gravel bed (Bolla Pittaluga et al., 2003). However, for small values of the Shields number the marginal curve displays an opposite trend, which is a consequence of the piecewise-form of the adopted transport function $\mathcal{G}$ (Equation 8), whose lower branch reduces to a simple power law. In this case, the coefficients $q_{\eta C}$ and $q_{\eta F}$ in Equation 24 are constant and the critical aspect ratio becomes inversely proportional to the square root of θ_{g0}. The minimum of the marginal curve basically corresponds to the value at which the mobility parameter for the coarse fraction crosses the threshold $\zeta = 1.35$.

Increasing the standard deviation of the sediment mixture, the Shields number corresponding to the minimum of the marginal curve also increases. As a consequence, the effect of sediment sorting on bifurcation stability highly depends on the value of θ_{g0}: for relatively small values of θ_{g0} the critical aspect ratio increases with σ_0, while for larger values the effect of sorting is almost negligible, but for the case of poorly sorted mixtures ($\sigma_0 = 2$), for which the critical aspect ratio undergoes a strong reduction.

To provide a physical interpretation of the effect of sorting on the critical aspect ratio, it proves useful to introduce the hypothesis that perturbations of the bed composition exert a minor effect on the total sediment transport, which implies that:

$$a_{12} + a_{22} \simeq 0. \tag{25}$$

In this case a simplified expression for the critical aspect ratio is readily obtained by summing the two Equation 17, which leads to:

$$\beta_{cr} = \frac{4r\alpha}{\sqrt{\theta_{g0}}} \frac{1}{2}\left(\frac{1}{\sqrt{l_{hrC}}} + \frac{1}{\sqrt{l_{hrF}}}\right) \frac{1}{\left[\left(q_{\eta C} + q_{\eta F}\right)/2 - 3/2 - c_D\right]}. \tag{26}$$

The appropriateness of this hypothesis is checked by comparing results of Equation 26 with those illustrated in Figure 3a, showing that the simplified expression is sufficient to capture the effect of increasing sediment heterogeneity (see Figure S6 in Supporting Information S1). Equation 26 highlights that the effect of mixed sediment on the stability of bifurcation depends on the role of the two terms within the parenthesis, which measure gravitational effects and variations in sediment transport capacity, providing the basis for the physical interpretation of Section 5.1.

Another useful information that can be deduced from the linear analysis is the relative importance of the perturbations of depth and grain composition, which can be quantified by differentiating Equation 17:

$$\hat{f}_C = \frac{1}{a_{12} - a_{22}}\left[\frac{4r\alpha}{\beta_{cr}\sqrt{\theta_{g0} l_{hrC}}}\left(\frac{1}{\sqrt{l_{hrC}}} - \frac{1}{\sqrt{l_{hrF}}}\right) - \left(q_{\eta C} - q_{\eta F}\right)\right]\hat{D}. \tag{27}$$

Considering a unitary depth perturbation (i.e., $\hat{D} = 1$) this gives the result illustrated in Figure 3b, which shows how the deeper branch (i.e., the one carrying the largest amount of flow and sediment) is in general characterized by bed coarsening, except for a small range of θ_{g0} values.

4. Equilibrium Configurations

The linear analysis presented above provides information about the critical point and on the relative amplitude of the small perturbations in a small neighborhood of the critical state. However, to obtain a complete overview of the equilibrium solutions the fully nonlinear problem (15a–15f) needs to be solved.

Model outputs are here analyzed in terms of different dimensionless asymmetry indexes:

$$\Delta Q = \frac{q_1 - q_2}{2q_0}, \quad \Delta Q_{s\phi} = \frac{f_1 q_{s1\phi} - f_2 q_{s2\phi}}{f_1 q_{s1\phi} + f_2 q_{s2\phi}}, \quad \Delta f_\phi = \frac{f_1 - f_2}{f_1 + f_2}, \tag{28}$$

which measure the deviation from a balanced configuration, and span between -1 and $+1$. Specifically, the asymmetry indexes (28) can be taken as representative indicators of the bifurcation response in terms of flow distribution (ΔQ), fractional sediment partition ($\Delta Q_{s\phi}$), and size composition (Δf_ϕ) of downstream channels. These outputs are then examined as a function of the distance from critical conditions, which can be measured through the following parameter:

$$\epsilon = \frac{\beta_0 - \beta_{cr}}{\beta_{cr}}, \tag{29}$$

which takes positive or negative values depending on the main channel falling under subcritical or supercritical conditions.

Equilibrium diagrams are shown in Figures 4 and 5, where the asymmetry indexes defined in Equation 28 are compared against the scaled aspect ratio ϵ for different degrees of sediment heterogeneity. Due to the geometrical symmetry of the problem, just one equilibrium configuration can be studied, say the case where channel 1 carries most of water and sediment (i.e., $\Delta Q > 0$). As in the uniform sediment case (i.e., $\sigma_0 = 0$) described by BRT, for $\epsilon > 0$ the balanced configuration (i.e., $\Delta Q = 0$) is unstable, and the system attains a stable steady state

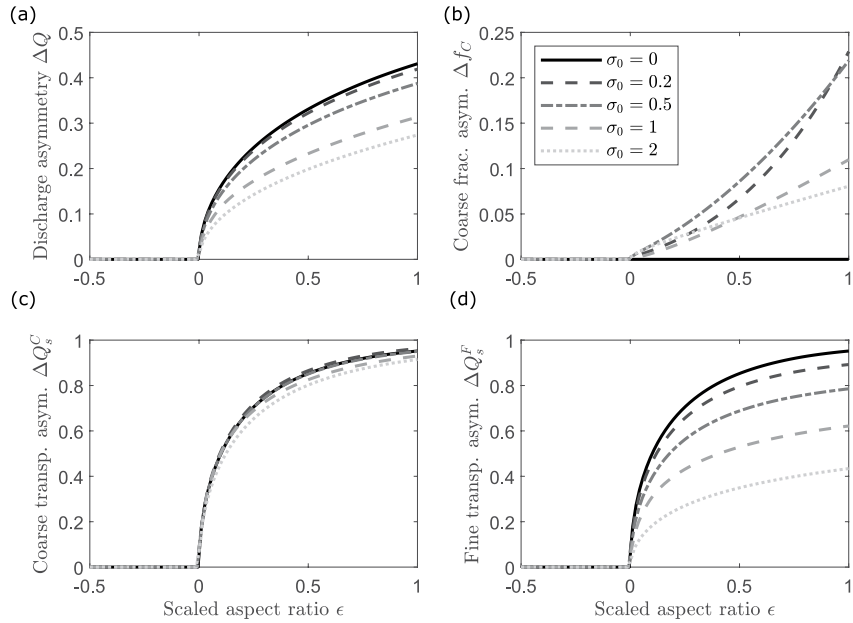

Figure 4. Equilibrium diagrams, where the different asymmetry indexes are compared against the reduced aspect ratio ϵ. The outcomes are displayed in terms of (a) ΔQ, (b) Δf_C, (c) ΔQ_{sC}, and (d) ΔQ_{sF}, for different values of the standard deviation σ_0. Fixed parameters are: $\theta_{g0} = 0.07$, $d_{g0} = 0.02$.

characterized by an unequal discharge distribution (Figure 4a), whose degree of asymmetry increases with ϵ. In addition, the unbalanced solution is characterized by a variation of the surface composition in the two branches. Specifically, when increasing ϵ the model shows a progressive coarsening of the dominant branch with respect to less carrying channel, as shown by the trend of Δf_C (Figure 4b). The degree of asymmetry of the solution is

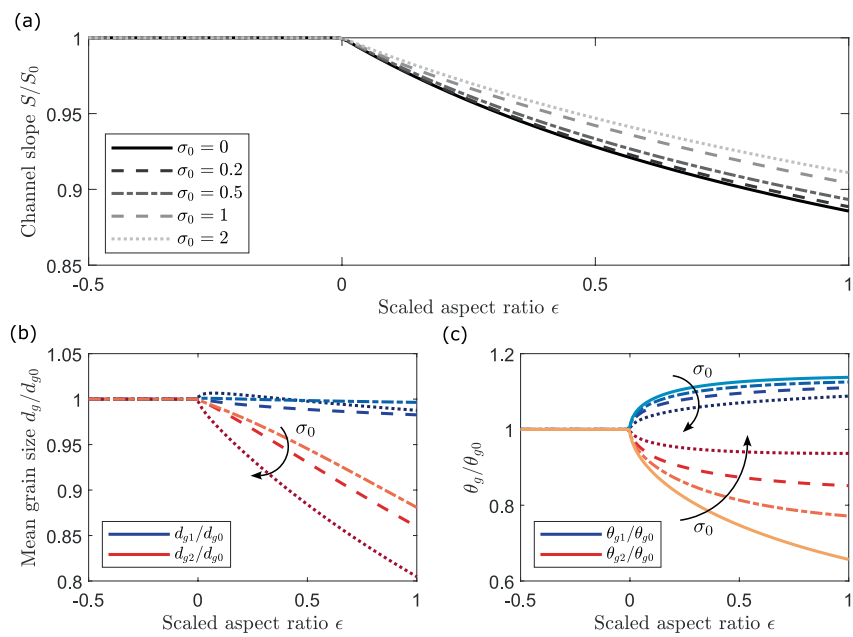

Figure 5. Equilibrium diagrams, where the downstream (a) relative channel slope S/S_0, (b) mean grain size d_g/d_{g0}, and (c) Shields mobility number θ_g/θ_{g0} of the individual branches are shown against the scaled aspect ratio ϵ for different values of the standard deviation σ_0. In panels (b, c), the continuous lines stand for the uniform case (i.e., $\sigma_0 = 0$), while dashed lines denote different values of σ_0 according with the symbolism employed in (a). Blue and red tones indicate the most-carrying and less-carrying channel, respectively. Fixed parameters are: $\theta_{g0} = 0.07$, $d_{g0} = 0.02$.

found to generally reduce when considering an heterogeneous mixture. Specifically, for increasing values of σ_0 the model predicts a systematic decrease of the discharge asymmetry ΔQ and an overall tendency toward a decrease of Δf_C.

The combined effect of the variations of ΔQ and Δf_C are associated with an asymmetric distribution of the sediment fluxes (Figures 4c and 4d). Due to the strong nonlinear relationship between the transport function and flow conditions, $\Delta Q_{s\phi}$ sharply increases with ϵ. However, while the effect of sorting on ΔQ_{sC} is fairly weak, a strong reduction of the fine fraction partition is predicted by the model. Consequently, the outcomes suggest that while the coarse fraction is almost entirely carried by the channel capturing the largest amount of flow, sediment sorting lets the penalized branch to carry a considerable fraction of fine material.

Recalling that in the BRT formulation the bifurcates have the same bed slope at equilibrium, Figure 5a shows that greater values of the standard deviation are followed by a drop of the channel slope. Moreover, when the mean grain size distribution is analyzed (Figure 5b), it can be appreciated the substantial fining occurring in the lowest-carrying branch, while the dominant branch retains nearly the same distribution with respect to the main thread. As a net result, the average grain size of the two branches is always lower than the feeding channel, to the point that for sufficiently wide channels both branches show a bed composition that is finer than that imposed upstream, as it will be discussed in Section 5.3. The variation of grain size composition is in turn associated with a modification of the transport capacity as compared to the uniform case. In particular, as illustrated in Figure 5c, the progressive fining substantially increases the mobility of the less-carrying branch.

As mentioned earlier, the above findings are obtained by considering the Wilcock and Crowe (2003) formulas. However, it is worth observing that the trends showed by the model outcomes are qualitatively reproduced even if other transport predictors and relations for hiding function are chosen (see Figures S1 and S2 in Supporting Information S1).

5. Discussion

5.1. Physical Interpretation of Model Results

Model results presented above show that grain sorting can affect the stability of channel bifurcations. The quantification of this effect through the linear analysis of the governing system (15a–15f) provides an expression for the critical aspect ratio that can be regarded as an extension of existing formulas to the case of mixed sediment. As in the case of uniform bed material, critical conditions occur when there exists a balance between sediment transport capacity and sediment supply, where the latter depends on the gravitational effect due to lateral bed slope. This balance is affected by the presence of a mixed sediment, which (a) increases the effectiveness of the gravitational mechanism, thus exerting a stabilizing effect; (b) increases the sensitivity of the sediment transport capacity to variations of water depth, then contributing to destabilize the system. Specifically, in the simplified expression for the critical aspect ratio (26) the term:

$$\frac{1}{2}\left(\frac{1}{\sqrt{l_{hrC}}}+\frac{1}{\sqrt{l_{hrF}}}\right), \tag{30}$$

which is equal to one for a uniform sediment composition, tends to grow with σ_0, indicating that the presence of a sediment mixture increases the overall magnitude of the gravitational effect. Similarly, the term at the denominator:

$$\left(q_{\eta_C}+q_{\eta_F}\right), \tag{31}$$

which measures the sensitivity of the total sediment transport to variations of Shields number, also tends to increase. This depends on the fact that the lower mobility of the coarse fraction enhances the nonlinearity of the response (i.e., q_{η_C} increases with σ_0). The higher mobility leads to an opposite effect for the fine sediment transport (i.e., q_{η_F} decreases with σ_0), but the latter term is less important because the fine fraction is closer to equimobility conditions. For relatively low values of Shields number the gravitational mechanism prevails on the enhanced sensitivity of the sediment transport, leading to the increase of β_{cr} illustrated in Figure 3a. On the other side, the second mechanism tends to prevail when θ_{g0} is higher, at least when the sediment is poorly sorted ($\sigma_0 \simeq 2$).

The linear analysis also allows for determining the variation of the bed surface composition represented by $\hat{f}_C$, as indicated by Equation 27. Again, the result depends on two opposite effects related to the gravitational mechanisms and to the transport capacity of the downstream channels. Specifically, the term:

$$\frac{1}{2}\left(\frac{1}{\sqrt{l_{hrC}}}-\frac{1}{\sqrt{l_{hrF}}}\right), \tag{32}$$

which represents the net result of gravitational selection, is always positive as the coarse fraction tends to be more subject to lateral deflection. Similarly, the term:

$$\left(q_{\eta C}-q_{\eta F}\right), \tag{33}$$

which represents selective transport in the downstream branches, is also positive, thus indicating that the coarse fraction is more sensitive to variations of bottom stress. Since the sign of $\hat{f}_C$ turns out to be almost negative over a wide range of mobility conditions, the bed composition in the downstream branches is mainly driven by the selection induced by the differential effect of gravity on the lateral deflection of the two fractions just upstream the bifurcation.

In addition, the model shows that when the channel β exceeds the critical value β_{cr}, the trivial, balanced solution, is no longer stable. In this case, it is found that the system evolves toward unbalanced equilibrium state solutions characterized by uneven discharge distribution and different bed surface composition in the downstream branches. This marks a clear difference with respect to the previous work of Schielen and Blom (2018), who found that stable equilibrium conditions are either balanced, with no asymmetry of discharge and bed composition, or characterized by a complete closure of one of the two branches.

The bedload transport asymmetry of unbalanced equilibrium states appears markedly reduced with respect to the case of uniform sediment. On the one side, this effect appears rather weak when looking at the coarse halve of sediment load, which is explained by considering that when increasing σ_0 there is more flow toward the less-carrying branch, but the associated increase of q_{sC} is mitigated by the reduction of the fractional content of coarse material. On the other side, the effect of sorting on the fine transport is rather strong. Specifically, when the heterogeneity is sufficiency large, we observe a variation in the order of +50% in the less-carrying branch, which results from the concordant effect of more flow and more fractional content of fine material. This indicates that the fining process can highly contribute to keep the penalized branch morphodynamically active (i.e., able to transport sediment) even when it carries a small fraction of the total flow. The capture of the largest coarse content by the most-carrying branch, along with the fining of the penalized bifurcate, are two factors that make the differential mobility between channels much more subdued than would be expected in the homogeneous sediment case (see Figure 5c).

5.2. The Effect of Hiding on Lateral Transport

One of the key ingredients of our model is represented by the nodal-point relation (7). The equation incorporates, although in a simplified manner, a fundamental mechanism for topographic sorting, namely the differential effect of the gravitational force on the bedload transport of the different fractions. A fundamental assumption adopted in the analysis consists in having neglected the contribution of hiding on the lateral direction (i.e., hypothesis of lateral gradation independence). The motivation behind our choice is essentially twofold: first, there is not a solid and univocal agreement in the literature whether hiding quantitatively affects the lateral movement of sediment on a sloping plane; second, the model outcomes in the gradation independence assumption on the gravitational terms qualitatively match field and laboratory observations (see Figure S7 in Supporting Information S1). Specifically, the outcomes discussed in Section 4 are comparable with the field observations of Burge (2006) and the laboratory experiments performed by Hirose et al. (2003), who reported bed coarsening in the most-carrying branch just downstream the bifurcation. Nonetheless, in the absence of a clear understanding of lateral sorting, it is instructive to further investigate the behavior of the model by introducing the effect of lateral hiding through the functional l_{hr} (Equation 7). Moreover, we find interesting to analyze what would be the effect of the extreme hypothesis of considering full equimobility of the two fractions within the branches (i.e., $g_{hr}=1$), as for example, assumed by Schielen and Blom (2018), who, however, did not account for the gravitational effect.

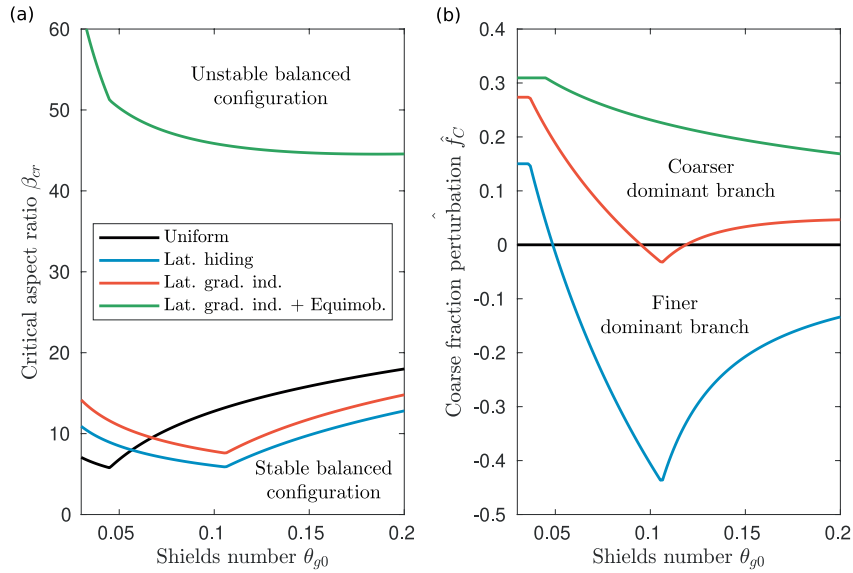

Figure 6. Outcomes of linear analysis depending on reference Shields number θ_{g0} for different modeling assumptions on lateral and streamwise sediment transport: lateral hiding (blue lines), lateral gradation independence (red lines), equimobility (green lines), with black lines denoting the homogeneous case. (a) Critical aspect ratio β_{cr}; (b) perturbation of the coarse fraction $\hat{f}_C$ in the dominant channel, for a unitary depth perturbation $\hat{D} = 1$. The plots are shown for $d_{g0} = 0.02$.

As illustrated in Figure 6a, considering the effect of lateral hiding invariably leads to a modest decrease of the critical aspect ratio. This can be explained by considering that lateral hiding tends to reduce the stabilizing gravitational term (expression 30), which widens the region of instability. An opposite effect is noticed when introducing the hypothesis of equimobility of sediment transport within the branches: in this case the destabilizing effect of sorting on the term (expression 31) vanishes. This leads to a dramatic increase of the critical aspect ratio, to the point that if this hypothesis was fulfilled most natural bifurcations would show stable balanced solutions, at least in the absence of external forcing factors.

The effect of lateral hiding is more evident when considering the perturbation of coarse fraction (Figure 6b). Specifically, the perturbation $\hat{f}_C$ becomes predominantly negative across the entire range of θ_{g0}, thus indicating a fining of the dominant branch. This can be explained again by considering that lateral hiding reduces the importance of the gravitational selection (expression 32), so that the term related to the selective transport (expression 33) prevails. An opposite trend is again observed when considering equimobility, as in this case the effect of selective transport identically vanishes.

Finally, as illustrated in Figures 7a and 7b, the discharge asymmetry and channel slope (and therefore bed elevation) are poorly affected by the choice of the lateral hiding function. Conversely, the above-mentioned effect of lateral hiding on the selection of bed surface composition leads the dominant channel to become slightly finer than the other bifurcate, an opposite trend with respect to the case of gradation independence (Figure 7c). Yet, the effect on grain size distribution is so small that bed composition in both branches is nearly equivalent to the feeder channel, suggesting that a distinct sorting pattern is almost absent when lateral hiding is retained. This leads the downstream transport capacities to be much closer to the uniform sediment case (Figure 7d). Consequently, the transport of fine material in the lowest-carrying distributary is significantly reduced (Figure 7f), while the transport of coarse material slightly increases (Figure 7e).

As a final step, the equilibrium solutions under the assumption of equal mobility are analyzed. First, results of Figure 7a show how the resulting discharge distribution becomes highly asymmetrical. This is consistent with the result of Figure 4a, in which higher values of σ_0 lead to an increasingly different mobility of the two fractions, which is associated with a reduced asymmetry. The strong coarsening of the dominant channel (Figure 7c) is again consistent with the results of linear analysis (Figure 6b). Interestingly, this coarsening is sufficient to compensate the increase of discharge asymmetry, so that the downstream transport capacities are almost unaffected by the choice of equimobility when compared against the case of lateral gradation independence (Figure 7d).

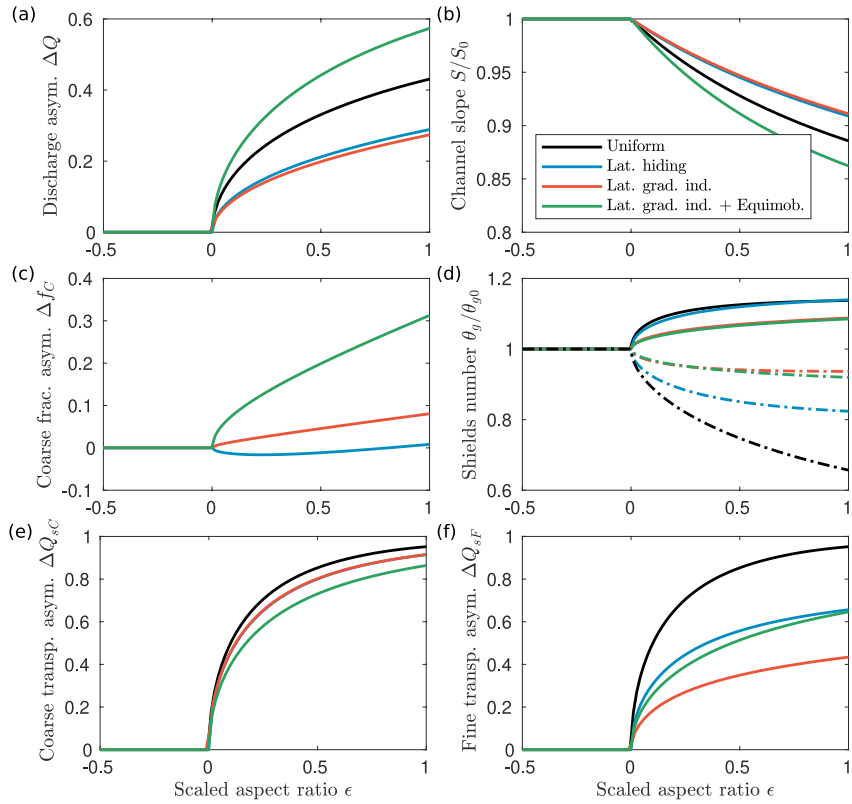

Figure 7. Comparison between the different modeling assumptions on lateral and streamwise sediment transport: lateral hiding (blue lines), lateral gradation independence (red lines), equimobility (green lines). Black lines denote the homogeneous case. (a) Discharge asymmetry ΔQ, (b) relative channel slope S/S_0, (c) coarse fraction asymmetry Δf_C, (d) scaled Shields number θ_g/θ_{g0}, and (e, f) transport asymmetries $\Delta Q_{s\phi}$ are plotted against the scaled aspect ratio ϵ. In panel (d) continuous and dotted lines stand for the most and less carrying branch, respectively. Reference parameters are: $\theta_{g0} = 0.07$, $d_{g0} = 0.02$, and $\sigma_0 = 2$.

5.3. Implications for Downstream Fining in Multi-Thread Rivers

The analysis suggests that at equilibrium both downstream branches are overall finer than the upstream feeder channel, as shown in Figure 8. Specifically, the resulting fining turns out to be almost independent of the reference Shields number, and weakly affected by the reference bed surface grain size (not shown). While results may appear to violate the mass conservation, this is clearly not the case, as the quantity that is conserved coincides with the transport fluxes, and not the bed surface composition. With this in mind, the overall fining can be interpreted as follows. The uneven distribution of discharge by the bifurcation increases the overall efficiency of the sediment transport, so that a gentler slope is sufficient to ensure the conservation of the total sediment flux. This is the typical behavior of braided channel networks, in which the heterogeneous distribution of the shear stress across the river leads to a strong increase of the sediment flux (R. I. Ferguson, 2003; Paola, 1996). However, the coarse fraction is naturally more sensitive to shear stress variations, so that its transport would be enhanced even more than the total flux. To compensate that increase, the fractional content of the coarse fraction needs to reduce, thus leading to the observed overall fining.

The foregoing analysis allows to cast an analogy with the problem of downstream fining in multi-thread rivers. Indeed, it has been observed that the bed texture of braided rivers is often characterized by sediment patches, which can be interpreted as spatial variations of the mean grain size across the reach (e.g., Lisle & Madej, 1992; Paola & Seal, 1995). These patches are associated with reach-averaged variation of the shear stress, and are able to produce a significant fining even in relative short reaches (e.g., R. Ferguson & Ashworth, 1991; Seal & Paola, 1995). Furthermore, a short-range downstream fining has been observed in a braided stretch of the Ridanna Creek, Italy, by Zolezzi et al. (2006), despite the authors did not analyze the cross-sectional size distribution in detail.

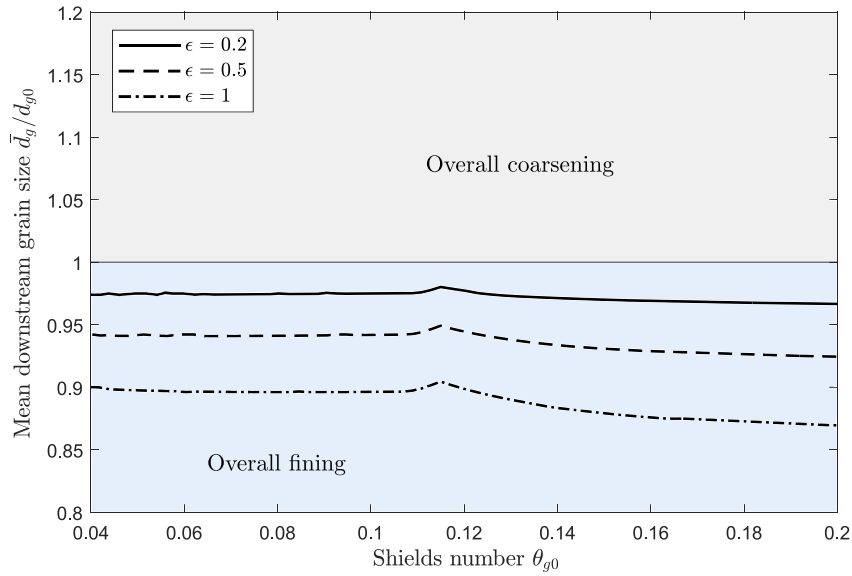

Figure 8. The mean surface grain size $\bar{d}_g = \left(d_{g1} + d_{g2}\right)/2$ of the distributaries, as scaled by the reference value d_{g0}, is plotted against the Shields number θ_{g0} for different values of ϵ. Fixed parameters are: $d_{g0} = 0.02$, and $\sigma_0 = 2$.

The lateral variation of grain size is thus a source for selective sorting and downstream fining that, as Paola and Seal (1995) discussed, it is independent of the relative mobility of different fractions in a mixture. In other words, a strong selective deposition can occur even if local equal mobility is satisfied. In a multi-thread river, several factors are sources of patches generation. For example, bars produce local variation of the magnitude and direction of sediment transport. In braided rivers, bars are known to be one of the main mechanisms for the formation of channel bifurcation (e.g., Ashmore, 1991, 2013; Repetto et al., 2002).

Following the line of thought drawn by Paola and Seal (1995), the sorting model of channel bifurcation presented here can be conceived through the following ideal experiment: a semi-infinite wide flume is assumed to carry, at equilibrium, a bimodal mixture with a size distribution that is spatially uniform. In addition, let equal mobility be enforced. At a certain point, in the middle of the flume a wall splits the flow between two smaller channels, which can be thought, in terms of grain size, as two grain patches. Despite the different fractions are assumed to be transported locally at the same rate, local variation in the mean grain size can exist. The lateral size variation is controlled by topographic sorting, specifically by the gravitational effect on sediment transport due to the transversal bed slope upstream the bifurcation.

In our analysis we refer to typical gravel-bed, bedload-dominated rivers. Hence, the present formulation is not conceived to model grain sorting in suspension-dominated, sand-bed streams, where different mechanisms are expected to become relevant. Specifically, turbulence is likely to promote the downstream transport of the finer fraction at the expense of the coarser counterpart, by driving the lighter particles toward the core region of the flow (Parker, 2008). This notwithstanding, present results may offer some insights for the interpretation of the downstream fining observed in coastal deltaic environments characterized by mixtures of both sand and gravel. An example is provided by the Selenga Delta (Russia), which is characterized by a strong downstream fining moving from the delta apex over 35 km of the delta topset, showing variations of d_{g0} up to three orders of magnitude (Dong et al., 2019). This progressive fining of bed material is associated with a decrease of the channels slope as flow is diverted between the branches, which is consistent with model results of Figure 5.

6. Conclusions

We propose a quasi-2D model to study equilibrium sorting at a channel bifurcation by extending the previous modeling framework of Bolla Pittaluga et al. (2003) to account for the presence of a heterogeneous sediment mixture, as typically the case of gravel bed rivers. Differently from the model recently proposed by Schielen and Blom (2018), sorting is here accounted for through a fully physically based description of the topographic effect

exerted by the bifurcation and the selective sediment transport within the branches. Model results allow us to draw the following conclusions:

1. The presence of a sediment mixture can influence the bifurcation in two opposite ways, depending on its effect on the two main mechanisms that control the stability of the bifurcation: (a) the gravitational pull due to the lateral slope upstream the bifurcation (stabilizing mechanism), and (b) variations of sediment transport capacity in the downstream channels (destabilizing mechanism). The presence of heterogeneous sediments tends to increase the effectiveness of both mechanisms, so that the net effect depends on the specific hydraulic conditions. In particular, for relative low values of the Shields number the presence of mixed sediment promotes the stability of the system, while for moderate mobility conditions there is a widening of the instability region (i.e., a decrease of the critical width-to depth ratio) when the sediment mixture becomes poorly sorted.
2. When the width-to-depth ratio exceeds a critical threshold, our model predicts the formation of unbalanced but stable equilibrium solutions, characterized by uneven discharge distribution and different bed surface composition in the downstream branches. The degree of discharge asymmetry tends to be lower than in the case of uniform sediment, and it decreases with the heterogeneity of the mixture.
3. The gravitational effects and the differential sediment transport capacity produce a selection of the two fractions. Specifically, the gravitational pull induces a coarsening of the dominating branch, while selective sediment transport has an opposite effect. Considering the hypothesis of lateral gradation independence, the gravitational mechanism tends to prevail, leading to a coarser bed composition in the dominating channel and a fining of the other branch. This trend is in qualitatively agreement with available laboratory and field observations.
4. The combined effect of reducing discharge asymmetry and bed surface fining tends to highly increase the transport of fine material in the penalized branch, while the greatest amount of the coarse fraction is always captured by the dominating branch. As a net result, relatively to the case of uniform sediment, the total sediment transport asymmetry is predicted to significantly reduce, contributing to maintain both branches morphologically active even at large values of the width-to-depth ratio, and therefore hampering the closure of the less-carrying branch.
5. The present analysis suggests that a bifurcating system is able to produce an overall fining of bed material in the downstream branches.

Ultimately, this work provides a first description of the key sorting mechanisms occurring at gravel-bedded river bifurcations, constituting a basic tool for the analysis and interpretation of laboratory and field measurements of sediment patchiness across multi-thread rivers.

Appendix A: Closure Relations for the Hiding Function

Different expressions for the hiding function g_{hr} have been proposed in the literature. The seminal Egiazaroff (1965) relation, as later modified by Ashida and Michiue (1972), reads as follows:

$$g_{hr} = \begin{cases} \left(\frac{d_g}{d}\right)\left[1 + 0.782\log_{10}\left(\frac{d}{d_g}\right)\right]^2, & d/d_g \geq 0.4 \\ 1/0.843, & d/d_g < 0.4. \end{cases} \quad \text{(A1)}$$

Alternatively, the reduced hiding function is often expressed by means of the following simple monomial form (e.g., Parker, 1990):

$$g_{hr} = \left(\frac{d}{d_g}\right)^{-b}, \quad \text{(A2)}$$

where field data indicated that the exponent b ranges approximately from 0 to 0.55 (Lanzoni & Tubino, 1999). Another widely used expression was proposed by Wilcock and Crowe (2003), who suggested to adopt a variable exponent, given by the expression (see Equations 8a and 8b):

$$b = \frac{0.67}{1 + \exp(1.5 - d/d_g)}. \quad \text{(A3)}$$

The surface-based relation of Wilcock and Crowe (2003) has its main advantage in the fact that was experimentally calibrated taking into account grain sizes ranging from the gravel to sand domain.

A comparison among the different expressions for g_{hr} is provided in Figure A1.

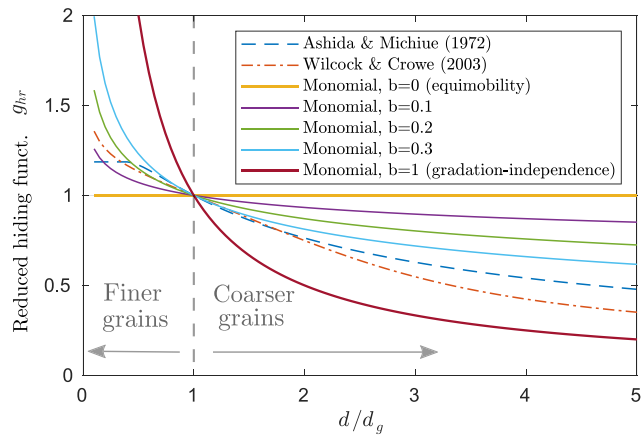

Figure A1. Reduced hiding function g_{hr} against the relative grain size d/d_g according to different expressions proposed in the literature.

List of Symbols

The next list describes the main symbols used within the body of the paper. Note that any subscript $_i$, with $i = 0$, 1, 2, indicates that the defined quantity refers to the upstream channel (if $i = 0$) or one of the two downstream branches (if $i = 1, 2$). Similarly, any subscript $_j$, with $j = F, C$, indicates that the defined quantity refers to the fine (F) or coarse (C) component of the bimodal sediment mixture. Finally, the hat over a given variable X indicates its linear expansion.

β_0	half width-to-depth ratio or aspect ratio of the upstream channel
β_{cr}	critical aspect ratio
ΔQ, ΔQ_{sj}, Δf_j	asymmetry indexes of the dimensionless fluid discharge, solid discharge and probability density function of the j sediment fraction, respectively
Δ	relative submerged weight of sediments
δ	order of magnitude of the perturbations
ϵ	parameter measuring the distance from the critical conditions in terms of the aspect ratio
η_i	bed elevations at the inlet of the $i = 1, 2$ downstream branch
$\mathcal{G}$	transport function
ϕ	sedimentological grain size scale
ϕ_{mi}	mean sedimentological grain size
ρ	water density
σ_{gi}	geometric grain size standard deviation of the mixture
τ_i	bottom shear stress
θ_{gi}	Shields mobility number of the mean grain size
θ_r	reference value of the Shields number for sediment motion relative to size d_{g0}
α	dimensionless length of the bifurcation cell
c_i	dimensionless Chézy coefficient
d	grain size
d_{gi}	geometric mean grain size of the mixture
D_i	flow depth
f_{ij}	grain size probability density distribution
g	gravitational acceleration
$g_{hr\phi}$	reduced hiding function
k_s	roughness height

$l_{hr\phi}$	function accounting for the possible hiding effect on the transversal sediment exchange
q_i	flow discharge per unit width
q_{sij}	volumetric sediment flux per unit width
q_{syj}	lateral solid discharge per unit width
q_y	lateral fluid discharge per unit width
r	Ikeda parameter
S_i	channel slope
W_i	channel width

Data Availability Statement

The MATLAB code used for this study is publicly available at (Ragno & Redolfi, 2023): https://doi.org/10.5281/zenodo.8146319.

Acknowledgments
This work has been supported by the Italian Ministry of Education, University and Research (MIUR) in the frame of the "Departments of Excellence" Grant L. 232/2016, by "Agenzia Provinciale per le Risorse Idriche e l'Energia" (APRIE) of the Province of Trento (Italy), and by the consortium iNEST (Interconnected North-Est Innovation Ecosystem) funded by the European Union Next-GenerationEU (Piano Nazionale di Ripresa e Resilienza (PNRR)—Missione 4 Componente 2, Investimento 1.5—D.D. 1058 23/06/2022, ECS_00000043). The comments and helpful suggestions by Associate Editor and three anonymous reviewers are greatly acknowledged.

References

Ashida, K., & Michiue, M. (1972). Study on hydraulic resistance and bedload transport rate in alluvial streams. *Transaction of JSCE*, *206*, 59–69. https://doi.org/10.2208/jscej1969.1972.206_59

Ashmore, P. E. (1991). How do gravel-bed rivers braid? *Canadian Journal of Earth Sciences*, *28*(3), 326–341. https://doi.org/10.1139/e91-030

Ashmore, P. E. (2013). Morphology and dynamics of braided rivers. In J. Shroder & E. Wohl (Eds.), *Treatise on geomorphology* (Vol. 9, pp. 289–312). Elsevier Inc. https://doi.org/10.1016/B978-0-12-374739-6.00242-6

Ashworth, P. J., & Ferguson, R. I. (1989). Size-selective entrainment of bed load in gravel bed streams. *Water Resources Research*, *25*(4), 627–634. https://doi.org/10.1029/WR025i004p00627

Ashworth, P. J., Ferguson, R. I., Ashmore, P. E., Paola, C., Powell, D. M., & Prestegaard, K. L. (1992). Measurements in a braided river chute and Lobe 2. Sorting of bed load during entrainment, transport, and deposition. *Water Resources Research*, *28*(7), 1887–1896. https://doi.org/10.1029/92wr00702

Bolla Pittaluga, M., Repetto, R., & Tubino, M. (2003). Channel bifurcation in braided rivers: Equilibrium configurations and stability. *Water Resources Research*, *39*(3), 1–13. https://doi.org/10.1029/2001WR001112

Burge, L. M. (2006). Stability, morphology and surface grain size patterns of channel bifurcation in gravel-cobble bedded anabranching rivers. *Earth Surface Processes and Landforms*, *31*(10), 1211–1226. https://doi.org/10.1002/esp.1325

Colombini, M., & Parker, G. (1995). Longitudinal streaks. *Journal of Fluid Mechanics*, *304*, 161–183. https://doi.org/10.1017/S0022112095004381

Cordier, F., Tassi, P., Claude, N., Crosato, A., Rodrigues, S., & Pham Van Bang, D. (2019). Numerical study of alternate bars in alluvial channels with nonuniform sediment. *Water Resources Research*, *55*(4), 2976–3003. https://doi.org/10.1029/2017WR022420

Cui, Y., Parker, G., & Paola, C. (1996). Numerical simulation of aggradation and downstream fining. *Journal of Hydraulic Research*, *34*(2), 185–204. https://doi.org/10.1080/00221689609498496

Dong, T. Y., Nittrouer, J. A., Czapiga, M. J., Ma, H., McElroy, B., Il'icheva, E., et al. (2019). Roles of bank material in setting bankfull hydraulic geometry as informed by the Selenga river delta, Russia. *Water Resources Research*, *55*(1), 827–846. https://doi.org/10.1029/2017WR021985

Egiazaroff, I. V. (1965). Calculation of nonuniform sediment concentrations. *Journal of the Hydraulics Division*, *91*(4), 225–247. https://doi.org/10.1061/JYCEAJ.0001277

Einstein, H. A. (1950). *The bed-load function for sediment transportation in open channel flows (technical report)*. United States Department of Agriculture Soil Conservation Service. (Publication Title: Technical Bulletin Volume: 1026).

Ferguson, R. I. (2003). The missing dimension: Effects of lateral variation on 1-D calculations of fluvial bedload transport. *Geomorphology*, *56*(1–2), 1–14. https://doi.org/10.1016/S0169-555X(03)00042-4

Ferguson, R. I., & Ashworth, P. (1991). Slope-induced changes in channel character along a gravel-bed stream: The Allt Dubhaig, Scotland. *Earth Surface Processes and Landforms*, *16*(1), 65–82. https://doi.org/10.1002/esp.3290160108

Ferguson, R. I., Hoey, T., Wathen, S., & Werritty, A. (1996). Field evidence for rapid downstream fining of river gravels through selective transport. *Geology*, *24*(2), 179–182. https://doi.org/10.1130/0091-7613(1996)024⟨0179:FEFRDF⟩2.3.CO;2

Frings, R. M., & Kleinhans, M. G. (2008). Complex variations in sediment transport at three large river bifurcations during discharge waves in the river Rhine. *Sedimentology*, *55*(5), 1145–1171. https://doi.org/10.1111/j.1365-3091.2007.00940.x

Hasegawa, K., Fujita, T., Meguro, H., & Tatuzawa, H. (2000). Bed forms in steep channels with heterogeneous bed materials induced by bottom elevation instability and sorting instability. *Suikougaku Ronbunshuu*, *44*, 659–664. https://doi.org/10.2208/prohe.44.659

Hirano, M. (1971). River-bed degradation with armoring. *Transaction of JSCE*, *195*(11), 55–65. https://doi.org/10.2208/jscej1969.1971.195_55

Hirose, K., Hasegawa, K., & Meguro, H. (2003). Experiments and analysis on mainstream alternation in a bifurcated channel in mountain rivers. In A. Sanchez-Arcilla & A. Bateman (Eds.), *3rd IAHR symposium on river, coastal and Estuarine morphodynamics* (pp. 571–583). IAHR.

Hoey, T. B., & Ferguson, R. I. (1994). Numerical simulation of downstream fining by selective transport in gravel bed rivers: Model development and illustration. *Water Resources Research*, *30*(7), 2251–2260. https://doi.org/10.1029/94wr00556

Ikeda, S. (1982). Incipient motion of sand particles on side slopes. *Journal of the Hydraulics Division*, *108*(1), 95–114. https://doi.org/10.1061/jyceaj.0005812

Ikeda, S. (1989). Sediment transport and sorting at bends. In *River meandering* (Vol. 12, pp. 103–125). American Geophysical Union. https://doi.org/10.1029/wm012p0103

Iseya, F., & Ikeda, H. (1987). Pulsations in bedload transport rates induced by a longitudinal sediment sorting: A flume study using sand and gravel mixtures. *Geografiska Annaler. Series A, Physical Geography*, *69*(1), 15–27. https://doi.org/10.1080/04353676.1987.11880193

Kästner, K., & Hoitink, A. (2019). Flow and suspended sediment division at two highly asymmetric bifurcations in a river delta: Implications for channel stability. *Journal of Geophysical Research: Earth Surface*, *124*(10), 1–23. https://doi.org/10.1029/2018JF004994

Kawai, S. (1991). *A study on flow and sediment discharge rates at a bifurcation in an open channel* (Doctoral dissertation). Kyoto University. https://doi.org/10.11501/2964438

Keulegan, G. H. (1938). Laws of turbulent flow in open channels. *Journal of Research of the National Bureau of Standards*, *21*(6), 707–741. https://doi.org/10.6028/jres.021.039

Kleinhans, M. G., Ferguson, R. I., Lane, S. N., & Hardy, R. J. (2013). Splitting rivers at their seams: Bifurcations and avulsion. *Earth Surface Processes and Landforms*, *38*(1), 47–61. https://doi.org/10.1002/esp.3268

Lanzoni, S., & Tubino, M. (1999). Grain sorting and bar instability. *Journal of Fluid Mechanics*, *393*(August), 149–174. https://doi.org/10.1017/S0022112099005583

Lisle, T. E., & Madej, M. A. (1992). Spatial variation in armouring in a channel with high sediment supply. In P. Billi, R. D. Hey, C. R. Thorne, & P. Tacconi (Eds.), *Dynamics of gravel-bed rivers* (pp. 277–293). John Wiley & Sons Ltd.

Meguro, H., Hasegawa, K., & Nakamura, K. (2002). Experimental study on bifurcated channel changes and sediment transport in a mountain river. *Proceedings of Hydraulic Engineering*, *46*, 755–760. https://doi.org/10.2208/prohe.46.755

Nelson, P. A., McDonald, R. R., Nelson, J. M., & Dietrich, W. E. (2015). Coevolution of bed surface patchiness and channel morphology: 1. Mechanisms of forced patch formation. *Journal of Geophysical Research: Earth Surface*, *120*(9), 1687–1707. https://doi.org/10.1002/2014JF003428

Olesen, K. W. (1987). *Bed topography in shallow river bends (Unpublished doctoral dissertation)*. University of Delft.

Paola, C. (1996). Incoherent structure: Turbulence as a metaphor for stream braiding. In P. J. Ashworth, S. J. Bennett, J. L. Best, & S. J. McLelland (Eds.), *Coherent flow structures in open channels*. John Wiley & Sons, Ltd.

Paola, C., Parker, G., Seal, R., Sinha, S. K., Southard, J. B., & Wilcock, P. R. (1992). Downstream fining by selective deposition in a laboratory flume. *Science*, *258*(December), 1757–1760. https://doi.org/10.1126/science.258.5089.1757

Paola, C., & Seal, R. (1995). Grain size patchiness as a cause of selective deposition and downstream fining. *Water Resources Research*, *31*(5), 1395–1407. https://doi.org/10.1029/94wr02975

Parker, G. (1990). Surface-based bedload transport relation for gravel rivers. *Journal of Hydraulic Research*, *28*(4), 417–436. https://doi.org/10.1080/00221689009499058

Parker, G. (1991a). Selective sorting and abrasion of river gravel. I: Theory. *Journal of Hydraulic Engineering*, *117*(2), 131–147. https://doi.org/10.1061/(asce)0733-9429(1991)117:2(131)

Parker, G. (1991b). Some random notes on grain sorting. In *International seminar on grain sorting* (pp. 19–76). Ascona.

Parker, G. (2004). 1D sediment transport morphodynamics with applications to rivers and turbidity currents. E-book available at Gary Parker's Morphodynamics Web Page.

Parker, G. (2008). Transport of gravel and sediment mixtures. In M. H. García (Ed.), *Sedimentation engineering* (pp. 165–251). ASCE. https://doi.org/10.1061/9780784408148.ch03

Parker, G., & Andrews, E. D. (1985). Sorting of bed load sediment by flow in meander bends. *Water Resources Research*, *21*(9), 1361–1373. https://doi.org/10.1029/WR021i009p01361

Parker, G., & Klingeman, P. C. (1982). On why gravel bed streams are paved. *Water Resources Research*, *18*(5), 1409–1423. https://doi.org/10.1029/wr018i005p01409

Parker, G., & Sutherland, A. J. (1990). Fluvial armor. *Journal of Hydraulic Research*, *28*(5), 529–544. https://doi.org/10.1080/00221689009499044

Parker, G., & Toro-Escobar, C. M. (2002). Equal mobility of gravel in streams: The remains of the day. *Water Resources Research*, *38*(11), 46-1–46-8. https://doi.org/10.1029/2001wr000669

Powell, D. M., Laronne, J. B., Reid, I., & Barzilai, R. (2012). The bed morphology of upland single-thread channels in semi-arid environments: Evidence of repeating bedforms and their wider implications for gravel-bed rivers. *Earth Surface Processes and Landforms*, *37*(7), 741–753. https://doi.org/10.1002/esp.3199

Powell, D. M., Reid, I., & Laronne, J. B. (2001). Evolution of bed load grain size distribution with increasing flow strength and the effect of flow duration on the caliber of bed load sediment yield in ephemeral gravel bed rivers. *Water Resources Research*, *37*(5), 1463–1474. https://doi.org/10.1029/2000WR900342

Qian, H., Cao, Z., Liu, H., & Pender, G. (2017). Numerical modelling of alternate bar formation, development and sediment sorting in straight channels. *Earth Surface Processes and Landforms*, *42*(4), 555–574. https://doi.org/10.1002/esp.3988

Ragno, N., & Redolfi, M. (2023). A tool for computing the equilibrium states of river bifurcations with heterogeneous sediment [Software]. Zenodo. https://doi.org/10.5281/zenodo.8146319

Ragno, N., Redolfi, M., & Tubino, M. (2021). Coupled morphodynamics of river bifurcations and confluences. *Water Resources Research*, *57*(1), 1–26. https://doi.org/10.1029/2020WR028515

Redolfi, M., Zolezzi, G., & Tubino, M. (2019). Free and forced morphodynamics of river bifurcations. *Earth Surface Processes and Landforms*, *44*(4), 973–987. https://doi.org/10.1002/esp.4561

Repetto, R., Tubino, M., & Paola, C. (2002). Planimetric instability of channels with variable width. *Journal of Fluid Mechanics*, *457*, 79–109. https://doi.org/10.1017/S0022112001007595

Schielen, R. M., & Blom, A. (2018). A reduced complexity model of a gravel-sand river bifurcation: Equilibrium states and their stability. *Advances in Water Resources*, *121*(July), 9–21. (Publisher: Elsevier Ltd). https://doi.org/10.1016/j.advwatres.2018.07.010

Seal, R., & Paola, C. (1995). Observations of downstream fining on the North Fork Toutle river near mount St. Helens, Washington. *Water Resources Research*, *31*(5), 1409–1419. https://doi.org/10.1029/94wr02976

Seminara, G., Colombini, M., & Parker, G. (1996). Nearly pure sorting waves and formation of bedload sheets. *Journal of Fluid Mechanics*, *312*(April), 253–278. https://doi.org/10.1017/S0022112096001991

Seminara, G., Solari, L., & Tubino, M. (1997). Finite amplitude scour and grain sorting in wide channel bends. In *Environmental and coastal hydraulics: Protecting the Aquatic habitat*. ASCE.

Singh, U., Crosato, A., Giri, S., & Hicks, M. (2017). Sediment heterogeneity and mobility in the morphodynamic modelling of gravel-bed braided rivers. *Advances in Water Resources*, *104*, 127–144. (Publisher: Elsevier Ltd). https://doi.org/10.1016/j.advwatres.2017.02.005

Sloff, K., & Mosselman, E. (2012). Bifurcation modelling in a meandering gravel-sand bed river. *Earth Surface Processes and Landforms*, *37*(14), 1556–1566. https://doi.org/10.1002/esp.3305

Sun, T., Meakin, P., & Jøssang, T. (2001). A computer model for meandering rivers with multiple bed load sediment sizes 1. Theory. *Water Resources Research*, *37*(8), 2243–2258. https://doi.org/10.1029/2000WR900397

Szewczyk, L., Grimaud, J.-L., Cojan, I., & Piégay, H. (2021). Bedload infilling and depositional patterns in chute cutoffs channels of a gravel-bed river: The Ain River, France. *Earth Surface Processes and Landforms*, *47*(2), 1–18. https://doi.org/10.1002/esp.5260

Wang, Z. B., De Vries, M., Fokkink, R. J., & Langerak, A. (1995). Stability of river bifurcations in 1D morphodynamic models. *Journal of Hydraulic Research*, *33*(6), 739–750. https://doi.org/10.1080/00221689509498549

Whiting, P. J., Dietrich, W. E., Leopold, L. B., Drake, T. G., & Shreve, R. L. (1988). Bedload sheets in heterogeneous sediment. *Geology*, *16*(2), 105–108. https://doi.org/10.1130/0091-7613(1988)016⟨0105:BSIHS⟩2.3.CO;2

Wilcock, P. R., & Crowe, J. C. (2003). Surface-based transport model for mixed-size sediment. *Journal of Hydraulic Engineering*, *129*(February), 120–128. https://doi.org/10.1061/(ASCE)0733-9429(2003)129:2(120)

Yamasaka, M., Ikeda, S., & Kizaki, S. (1987). Lateral sediment transport of heterogeneous bed materials. *Proceedings of JSCE*, *387*(II-8), 105–114. https://doi.org/10.2208/jscej.1987.387_105

Zolezzi, G., Bertoldi, W., & Tubino, M. (2006). Morphological analysis and prediction of river bifurcations. In G. H. Best, J. L. Bristow, & C. S. Petts (Eds.), *Braided rivers: Process, deposits, ecology and management* (Vol. 36, pp. 233–256). Blackwell. https://doi.org/10.1002/9781444304374.ch11